Atmos. Chem. Phys. Discuss., 14, 24221–24271, 2014
www.atmos-chem-phys-discuss.net/14/24221/2014/
doi:10.5194/acpd-14-24221-2014

Atmospheric Chemistry and Physics Discussions

Two years of near real-time chemical composition of submicron aerosols in the region of Paris using an Aerosol Chemical Speciation Monitor (ACSm) and a multi-wavelength Aethalometer

J.-E. Petit[1,2], O. Favez[1], J. Sciare[2], V. Crenn[2], R. Sarda-Estève[2], N. Bonnaire[2], G. Močnik[3], J.-C. Dupont[4], M. Haeffelin[4], and E. Leoz-Garziandia[1]

[1]Institut National de l'Environnement Industriel et des Risques, Verneuil-en-Halatte, France
[2]Laboratoire des Sciences du Climat et de l'Environnement (CNRS-CEA-UVSQ), CEA Orme des Merisiers, Gif-sur-Yvette, France
[3]Aerosol d.o.o., Ljubljana, Slovenia
[4]Laboratoire de Météorologie Dynamique, Institut Pierre Simon Laplace, Ecole Polytechnique, Palaiseau, France

Received: 22 July 2014 – Accepted: 2 September 2014 – Published: 18 September 2014

Correspondence to: O. Favez (olivier.favez@ineris.fr)

Published by Copernicus Publications on behalf of the European Geosciences Union.

ACPD
14, 24221–24271, 2014

Abstract

Aerosol Mass Spectrometer (AMS) measurements have been successfully used towards a better understanding of non-refractory submicron (PM_1) aerosol chemical properties based on short-term campaign. The recently developed Aerosol Chemical Speciation Monitor (ACSM) has been designed to deliver quite similar artefact-free chemical information but for low-cost, and to perform robust monitoring over long-term period. When deployed in parallel with real-time Black Carbon (BC) measurements, the combined dataset allows for a quasi-comprehensive description of the whole PM_1 fraction in near real-time. Here we present a 2 year long ACSM and BC datasets, between mid-2011 and mid-2013, obtained at the French atmospheric SIRTA supersite being representative of background PM levels of the region of Paris. This large dataset shows intense and time limited (few hours) pollution events observed during wintertime in the region of Paris pointing to local carbonaceous emissions (mainly combustion sources). A non-parametric wind regression analysis was performed on this 2 year dataset for the major PM_1 constituents (organic matter, nitrate, sulphate and source apportioned BC) and ammonia in order to better refine their geographical origins and assess local/regional/advected contributions which information are mandatory for efficient mitigation strategies. While ammonium sulphate typically shows a clear advected pattern, ammonium nitrate partially displays a similar feature, but less expected, it also exhibits a significant contribution of regional and local emissions. Contribution of regional background OA is significant in spring and summer while a more pronounced local origin is evidenced during wintertime which pattern is also observed for BC originating from domestic wood burning. Using time-resolved ACSM and BC information, seasonally differentiated weekly diurnal profiles of these constituents were investigated and helped to identify the main parameters controlling their temporal variations (sources, meteorological parameters). Finally, a careful investigation of all the major pollution episodes observed over the region of Paris between 2011 and 2013 was performed and classified in terms of chemical composition and BC-to-sulphate ratio used here as a proxy

ACPD
14, 24221–24271, 2014

of the local/regional vs. advected contribution of PM. In conclusion, these first 2 year quality-controlled measurements of ACSM clearly demonstrate their great potential to monitor on a long term basis aerosol sources and their geographical origin and provide strategic information in near real-time during pollution episodes. They also support the capacity of the ACSM to be proposed as a robust and credible alternative to filter-based sampling techniques for long term monitoring strategies.

1 Introduction

The understanding of the formation and fate of atmospheric particulate pollution in urban areas represents sanitary, scientific, economic, societal and political challenges, greatly amplified by increasing media coverage of pollution episodes all around the world. Growing evidences of adverse health effects of atmospheric pollutants (Chow et al., 2006; Pope and Dockery, 2006; Ramgolam et al., 2009; WHO, 2012) are illustrated by the fact that ambient air pollution has been characterized as carcinogenic since December 2013 by the International Agency for Research on Cancer (IARC, 2013). However, the "aerosol cocktail effect", directly linked to the complexity of the chemical composition and sources of the particulate phase, remains poorly understood.

In an effort to fill these lacks of knowledge, worldwide coordinated networking activities (such as Global Atmosphere Watch, European Monitoring and Evaluation Programme, AErosol RObotic NETwork) have been documenting, since decades, the chemical, physical and optical properties of aerosol pollution in various environments. At a European level, this effort is also supported by the Aerosols, Clouds and Traces gases Research InfraStructure network (ACTRIS) program which aims at pooling high quality data from state-of-the-art instrumentation such as the Aerosol Chemical Speciation Monitor (ACSM, Aerodyne Research Inc., Billerica, MA, USA).

The ACSM has been recently developed with the aim of robust and easy-to-use near real-time and artifact-free measurements of the major chemical composition of

ACPD
14, 24221–24271, 2014

non-refractory submicron aerosol (OM, NO_3^-, SO_4^{2-}, NH_4^+ and Cl^-) on long-term basis (Ng et al., 2011). In parallel, a growing interest is also dedicated worldwide for the monitoring of Black Carbon (BC), considered as an adequate indicator of potential anthropogenic emission having sanitary impacts (Janssen et al., 2011). In particular, the use of 7-wavelength Aethalometer (Magee Scientific, USA) allows furthermore for BC source apportionment (Sandradewi et al., 2008), proven as robust over long term period (Herich et al., 2011). The combination of measurements from both instruments may thus constitute an efficient and relatively low-cost tool for the monitoring of submicron aerosol chemistry and a better knowledge of their phenomenology. Such strategy may be particularly useful to document aerosol sources and their geographical origin in large urban environments such as large urban areas which are characterized by a complex mixture of gaseous and particulate pollutions. Paris (France) is one of the largest European megacities and is rather isolated from other major urban environments. With ∼ 11 million inhabitants, the Paris region accounts for 20 % of total French population distributed over only 2 % of its territory, leading to enhanced exposure to various types of pollution. Moreover, the flat orography of the Paris region favors pollution transport, making it representative of North-Western Europe aerosol pollution. AIRPARIF, the regional air quality monitoring network, recently estimated that, since 2007, about 2 million people per year have been exposed to poor air quality (referring to daily PM_{10} concentrations European limit values; AIRPARIF, 2014) in this region. Over the past 7 years, $PM_{2.5}$ yearly concentrations in Paris have remained quite stable although no continuous monitoring of the chemical composition of the particulate phase is available to investigate any trends in the major sources of fine aerosols.

A recent research program, based on a 1 year (2009–2010) daily filter sampling carried out at 5 various sites (traffic, urban, suburban and regional background; Ghersi et al., 2010), was a unique opportunity to give insight into the seasonal variations, sources and geographical origins of aerosol pollution in the region of Paris (Bressi et al., 2013a, b; Petetin et al., 2013). However, long-term monitoring strategies based on the chemical analysis of aerosols sampled on filters are subject to various sam-

ACPD
14, 24221–24271, 2014

pling and analytical artifacts (Appel et al., 1984; Turpin et al., 1994; Pathak et al., 2004; Cheng et al., 2009) and assumptions (OC-to-OM ratio for instance); they involve laborious laboratory analyses; they cannot capture processes governing diurnal variations of atmospheric pollutants and fail to provide rapid diagnostics during pollution events.

In this context, Aerosol Mass Spectrometer (AMS) techniques have provided extremely valuable information of artifact-free real-time chemical composition of submicron aerosols in urban areas over the past 10 years (Zhang et al., 2004, 2007; Jimenez et al., 2009). In Europe, organic matter (OM) and ammonium nitrate are generally the two main constituents of PM_1 (Zhang et al., 2007), showing, however, significant discrepancies during pollution episodes in terms of chemical composition. Real-time AMS data have improved the understanding of the physical and chemical (trans)formation pathways of both fractions, through the characterization of pollution dynamics and source apportionment analyses. Intensive field campaigns involving AMS measurements were performed during the 2009 summer and 2010 winter seasons in the frame of the European MEGAPOLI (Megacities: emissions, urban, regional and Global Atmospheric POLlution and climate effects, and Integrated tools for assessment and mitigation) research program. They greatly improved the understanding of the sources and transformation processes of Paris aerosols, and especially its submicron organic fraction (Crippa et al., 2013a, b, c; Freutel et al., 2013; Healy et al., 2012; Laborde et al., 2013; Healy et al., 2013; Zhang et al., 2014). However, AMS techniques cost, size and intensive control requirements make them impractical for unattended monitoring. Nevertheless, they may still represent the best strategy to investigate specific trends in aerosol sources, especially in the context of elevated and stable PM concentrations as observed over the region of Paris during the past few years. In that perspective, the recently commercialized ACSM may represent an interesting alternative and may ultimately represent the best strategy to deploy for long term monitoring of submicron aerosol sources and geographical origins.

As part of the ACTRIS project, a new in-situ atmospheric station has been implemented in 2011 at a background site of the region of Paris allowing the chemical,

ACPD
14, 24221–24271, 2014

physical and optical characterization of submicron aerosol pollution at a regional scale The key aim of the present paper is to describe and discuss one of the first long-term dataset obtained with the ACSM, offering opportunities for the evaluation of the scientific relevance of a new experimental strategy for long term monitoring of near real-time chemical composition of PM_1. Seasonal trends, wind sector analysis, diurnal variations and pollution episodes retrieved from a 2 year real-time measurement ACSM and BC datasets are presented and interpreted in order to refine the origins and parameters controlling the (trans)formation of particulate pollution over the region of Paris.

2 Material and methods

2.1 Sampling site and instrumentation

Long-term in-situ observations of the chemical, optical and physical properties of atmospheric aerosols have been initiated at SIRTA (Site Instrumental de Recherche par Télédétection Atmosphérique, http://sirta.ipsl.fr) since June 2011 within the EU-FP7 ACTRIS program (Aerosols, Clouds, and Traces gases Research InfraStructure Network, http://www.actris.net). Located 20 km Southwest of Paris (2.15° E, 48.71° N, 150 m a.s.l.) in a semi-rural area, this atmospheric supersite is representative of the regional background pollution over the region of Paris (Haeffelin et al., 2005; Crippa et al., 2013a).

The chemical composition of non-refractory submicron aerosol has been continuously monitored using a Quadripole Aerosol Chemical Speciation Monitor (Aerodyne Research Inc.) which has been described in details by Ng et al. (2011). Briefly, $PM_{2.5}$ aerosols are sampled at 3 L min^{-1} and then sub-sampled at 85 mL min^{-1} (volumetric flow) through an aerodynamic lens, focusing submicron particles (40–1000 nm aerodynamic diameter, A.D.) onto a 600 °C-heated conical tungsten vaporizer where non-refractory material are flash-vaporized and quasi-instantaneously ionized by electron impact at 70 eV. Fragments are detected following their mass-to-charge ratio by

ACPD
14, 24221–24271, 2014

a quadrupole mass spectrometer. The procedure followed for the retrieval of chemical species concentrations from ACSM measurements is fully described in the Supplement. Briefly, the instrument calibration has been performed following the recommendation of Jayne et al. (2000) and Ng et al. (2011), where generated mono-disperse 300 nm A.D. ammonium nitrate particles are injected into both ACSM and Condensation Particle Counter (CPC) at different concentrations. An average NO_3^- ionization efficiency of $2.72.10^{-11}$, as well as relative ion efficiencies (RIE) of 5.9, 1.2 and 1.4 for ammonium, sulphate and organic matter respectively, were used for the whole dataset. Collection efficiencies were corrected using algorithms proposed by Middlebrook et al. (2012), and data were finally cross-validated using collocated PM_1 as well as $PM_{2.5}$ urban background measurements, retrieved from the regional association of air quality monitoring (AIRPARIF, http://airparif.asso.fr). The PM_1 and $PM_{2.5}$ datasets were obtained using Tapered Element Oscillating Microbalances (TEOM) equipped Filter Dynamic Measurements Systems (FDMS) as described by Grover (2005). A total number of ~ 26 000 (30 min) ACSM data points were collected from June 2011 to June 2013 covering on average 92 ± 9 % of each month over this 2 year period (it is to note that September–October 2012 and February–March 2013 were not taken into account within the latter calculation because the instrument was used for short-term intensive campaigns at other locations).

Aerosol light absorption coefficients b_{abs} were retrieved every 5 min from a 7-wavelength (370, 470, 520, 590, 660, 880 and 950 nm) AE31 Aethalometer from June 2011 to February 2013, and from a 7-wavelength (370, 470, 520, 590, 660, 880 and 950 nm) AE33 Aethalometer from February 2013 to May 2013. In both cases, instruments sampled aerosols with a $PM_{2.5}$ cut-off inlet, operating at 5 L min^{-1}. Filter-based absorption measurements need to be compensated for multiple scattering in the filter matrix and for loading effects, using mathematical algorithms (Collaud Coen et al., 2010). While AE31 data were compensated using the corrections of Weingartner et al. (2003) as described in Sciare et al. (2011), the use of the Dual-Spot Technology® in the AE33 avoids the need of manual post-processing to compensate the data (Dri-

ACPD
14, 24221–24271, 2014

novec et al., 2014). Both instruments performed absorption measurements simultaneously during 7 days in February 2013 (Fig. S1a). Absorption coefficients at 880 nm showed a slope of 0.93 and a very satisfactorily r^2 (0.96, n = 3023 of 5 min data points). Black Carbon concentrations for the whole (2 year) dataset were then calculated from the absorption coefficient at 880 nm, with a mass absorption cross-section (MAC) of 8.8 $m^2\,g^{-1}$ (Fig. S1b), determined from the comparison with collocated filter measurements of elemental carbon (EUSAAR2 thermo-optical protocol, Cavalli et al., 2010). This value is close from the default input value implemented in the AE33 at 880 nm (7.77 $m^2\,g^{-1}$). Although still under discussion (Bond and Bergstrom, 2006; Cappa et al., 2012), such relatively high MAC values might be related to a possible encapsulation of soot particle by organic/inorganic compounds at our regional background site and to the presence of BC from wood burning emissions during wintertime, both leading to an increase of BC mass absorption efficiency (Liousse et al., 1993; Bond and Bergstrom, 2006; Lack et al., 2008). A total number of ~ 280 000 BC data points (~ 133 000 5 min points from AE31 and ~ 147 000 1 min points from AE33) were collected from June 2011 to June 2013.

Ammonia measurements during selected periods (mainly during the spring, winter and summer seasons) were carried out using an AiRRmonia (Mechatronics Instruments BV, the Netherlands). Based on the conductimetric detection of ammonium, gaseous ammonia is sampled at 1 L min^{-1} through a sampling block equipped with an ammonia-permeable membrane; a water counter-flow allows ammonia to solubilize in ammonium. A second purification step is applied by adding 0.5 mM sodium hydroxide, leading to the detection of ammonium in the detector block. The instrument has been calibrated regularly using solutions of 0 ppb and 500 ppb of ammonium. Two sets of sampling syringes ensure a constant flow throughout the instrument, but also create a temporal shift, estimated at 20 to 40 min by different studies (Cowen et al., 2004; Zechmeister-Boltenstern, 2010). In our case, this shift was set at 30 min.

Pre-fired 47 mm diameter quartz filters were sampled in $PM_{2.5}$ at the same location using a low-volume (1 $m^3\,h^{-1}$) sampler (Partisol Plus, Thermo Environment)

ACPD
14, 24221–24271, 2014

equipped with a volatile organic compounds active charcoal denuder. Four-hour filters and 24 h filters were discontinuously sampled respectively from 10 February 2012 to 2 March 2012 and during the period from August 2012 to April 2013. These filters were analyzed for their water-soluble inorganic (anions and cations) and elemental/organic carbon contents using respectively Ion Chromatography and Sunset OC/EC analyzer (EUSAAR2 thermal protocol), accordingly to Sciare et al. (2008) and Cavalli et al. (2010).

Finally, standard meteorological parameters (Temperature, Relative Humidity, Wind Speed and Direction) were obtained from continuous measurements at Ecole Polytechnique, located 4 km East of our station with an A100R Campbell Scientific cup anemometer for wind speed and a W200P weathervane for wind direction, at 10 m a.g.l. Additionally, the Boundary Layer Height (BLH) was derived from Pal et al. (2013) methodology. The attribution of the BLH was processed in combining diagnostic of the surface stability from high frequency sonic anemometer measurements and LIght Detection and Ranging (LIDAR) attenuated backscatter gradients from aerosols and clouds.

All measurements presented here are expressed in Coordinated Universal Time (UTC).

2.2 Urban background $PM_{2.5}$ measurements

Within the framework of mandatory air quality monitoring, urban background measurements are continuously being carried out in the region of Paris. Hourly $PM_{2.5}$ data were retrieved from the three stations representative of the Paris urban background (namely Bobigny, Gennevilliers and Vitry-sur-Seine). Datasets are available online upon request on http://airparif.asso.fr.

ACPD
14, 24221–24271, 2014

2.3 Backtrajectories and non-parametric wind regression

To illustrate air mass origin during specific pollution episodes, 72 h backtrajectories were calculated every 3 h from the PC based version of Hysplit (Draxler, 1999) with GDAS meteorological field data. Backtrajectories were set to end at SIRTA coordinates (48.71° N, 2.21° E) at 100 m a.g.l.

Non-parametric Wind Regression (NWR) is a smoothing algorithm (Henry et al., 2009) to alternatively display pollution roses, and has been already successfully applied to various atmospheric pollutants and pollution sources (Yu et al., 2004; Pancras et al., 2011; Olson et al., 2012). The objective is to estimate the concentration of a pollutant given any (θ, υ) couple (wind direction and speed, respectively), from measured variables.

$$E\left(\theta|\vartheta\right) = \frac{\sum_{i=1}^{N} K_1\left(\frac{\theta - W_i}{\sigma}\right) \cdot K_2\left(\frac{\vartheta - Y_i}{h}\right) \cdot C_i}{\sum_{i=1}^{N} K_1\left(\frac{\theta - W_i}{\sigma}\right) \cdot K_2\left(\frac{\vartheta - Y_i}{h}\right)}$$

Where E is the concentration estimate at a wind direction θ and speed υ; W_i, Y_i and C_i the wind direction, speed and atmospheric concentrations, respectively, measured at t_i; σ and h the smoothing factors; and K_1 and K_2 two kernel smoothing functions defined as:

$$K_1(x) = \frac{1}{\sqrt{2\pi}} \cdot e^{-0.5 \cdot x^2}, \quad -\infty < x < \infty$$

$$K_2(x) = 0.75 \cdot \left(1 - x^2\right), \quad -1 < x < 1 = 0$$

The choice of the two smoothing factors σ and h can be carried out using statistical calculations, although its empirical determination stays feasible, as final interpretation should not be changed. Here, σ and h were set to 7 and 1.5, similarly to Petit

ACPD
14, 24221–24271, 2014

et al. (2014). Finally, the equivalent of the wind rose is calculated from the probability density:

$$f(\theta,\vartheta) = \frac{1}{N\sigma h} \cdot \sum_{i=1}^{N} K_1\left(\frac{\theta - W_i}{\sigma}\right) K_2\left(\frac{\vartheta - Y_i}{h}\right)$$

where N the is the total number of points.

Due to higher measurement uncertainties in wind direction at low speeds, data associated with wind speeds lower than $1\,m\,s^{-1}$ were discarded, potentially inducing an underestimation of very local pollution events.

2.4 Source apportionment of carbonaceous aerosols

The measurement of aerosol absorption at multiple wavelengths is allowing for BC source apportionment. Organic molecules, especially Polycyclic Aromatic Hydrocarbons and Humic-Like Substances, strongly absorb in the UV and blue part of the light spectrum. Based on the fact that these compounds are primarily related to biomass combustion, the deconvolution of BC into two contributions: fuel fossil and wood burning (BC_{ff} and BC_{wb}, respectively) can be carried out (Sandradewi et al., 2008). Such source apportionment has already been successfully performed during intensive field campaigns areas as well as for long-term monitoring periods, frequently enlightening the significant contribution of wood burning to ambient BC concentrations during wintertime (Favez et al., 2009, 2010; Sciare et al., 2011; Herich et al., 2011; Crippa et al., 2013a). Here, the 470 nm and 880 nm channels were used, with an absorption Ångström exponent of 2.1 and 1.0 for pure wood burning and traffic, respectively, similarly to a previous work focusing on the February–March 2012 period of the same dataset (Petit et al., 2014).

The source apportionment of our organic aerosol data is not presented here although Positive Matrix Factorization applied to AMS or ACSM database is an efficient tool for the identification of organic aerosol primary sources and secondary formation

ACPD
14, 24221–24271, 2014

processes (see for instance Lanz et al., 2007; Jimenez et al., 2009; El Haddad et al., 2013; Carbone et al., 2013; Bougiatioti et al., 2014; Petit et al., 2014). Such a work will be reported elsewhere (Crenn et al., 2014) as important issues related to the seasonal variation of specific organic aerosol factor profiles have to be addressed in many details with a lot of sensitivity tests which are beyond the objectives of the present study.

3 Cross-validation of particulate chemical species concentrations

Figure 1 illustrates the temporal variations of chemical species concentrations used for the present study from June 2011 to May 2013. This extended duration highlights the robustness of used instruments, and in particular the ACSM which did not undergo any major failures over this 2 year period. The consistency of the concentrations of each chemical constituent retrieved from the ACSM has been checked via comparisons with filter measurements (Fig. 2) as well as a chemical mass closure of PM_1 (Fig. 3).

ACSM nitrate is very consistent with filter measurements, the slope of the linear regression being close to 1 (r^2 = 0.85, N = 147). No overestimation of ACSM nitrate is observed at high concentrations, which suggests the ability of the Middlebrook algorithm to properly correct our ACSM collection efficiencies. Higher discrepancies are observed for sulphate. This feature has already been mentioned in previous studies for ACSM (Ng et al., 2011; Budisulistiorini et al., 2014), and AMS instruments (Takegawa et al., 2005). This could be firstly related to the size distribution of sulphate, as fine ($PM_{2.5}$) sulphate can partially be associated with submicron sea salt and/or dust particles. Fine ammonium sulphate aerosols originating from secondary processes and long-range transport (Sciare et al., 2010; Freutel et al., 2013) may also present a larger size mode extending above 1 µm and partially not sampled by the ACSM. A sulphate ion efficiency calibration was also performed in May 2013 to investigate possible change in RIE, but no significant discrepancy from the default value of 1.2 was found.

The OM-to-OC ratio obtained from the comparison between ACSM and filter-based measurements exhibits a mean value of approximately 1.5, which is lower than the

ACPD
14, 24221–24271, 2014

value recommended for urban areas (1.6 ± 0.2, Turpin and Lim, 2001) and 33 % lower than and/or equal to values used in Paris metropolitan area in previous studies (~ 2 in Bressi et al., 2013; 1.6 in Sciare et al., 2010). Although this ratio is subject to caution, by virtue of potential geographical and temporal discrepancies, the relatively low value observed here might be explained by the presence of organic material between 1 and 2.5 µm as well as filter sampling artifacts.

A chemical mass closure exercise, where the combination of validated ACSM and Aethalometer data is compared to co-located PM_1 TEOM-FDMS measurements, was used to assess the capacity of the two former instruments to correctly describe the PM_1 fraction over long-term periods. For this purpose, the reconstructed PM_1 (PM_{chem}) introduced here corresponds to the sum of all non-refractory species measured by the ACSM (OM, NO_3^-, SO_4^{2-}, NH_4^+ and Cl^-) and Black Carbon measured by Aethalometer, and is assumed to quasi-exhaustively account for submicron aerosols (Putaud et al., 2004). PM_{chem} daily averages were compared to the TEOM-FDMS dataset, since the latter instrument is considered as equivalent to the gravimetric reference method on this temporal scale. From June 2011 to May 2013, the 341-point (this number being due to the combined availability of ACSM, BC and PM data) scatter plot shows a very satisfactorily correlation coefficient (r^2 = 0.85) with a slope of 1.06.

4 Representativeness of our 2 year observation period

Monthly mean atmospheric conditions were compared to standard meteorological parameters in order to investigate any anomalies over the 2011–2013 period (Fig. 4). Temperatures, rainfalls and sun exposure representative for the region of Paris were retrieved from monthly weather reports available at https://donneespubliques.meteofrance.fr, and are calculated from a 30 year period (1981–2010) (Arguez and Vose, 2011). A similar study was also performed for particulate matter concentrations, with representative $PM_{2.5}$ defined as the average $PM_{2.5}$ concentrations calculated from 2007 to 2014 at the three historical Airparif urban background stations.

ACPD
14, 24221–24271, 2014

Briefly, autumn 2011 was relatively mild, $PM_{2.5}$ levels being close to representative concentrations for the period. The end of winter 2011–2012 and early spring 2012 were particularly dry and sunny, enabling enhanced photochemical transformation and exhibited unusually high $PM_{2.5}$ concentrations in February and March 2012. The summer 2012 was chilly and rainy, especially in June 2012, leading to lower $PM_{2.5}$ levels (Yiou and Cattiaux, 2013). Finally, the first two months of 2013 were unusually cold, whereas March 2013 was remarkably representative of wintertime conditions. The highest observed discrepancies occur with highest measured mass, which may highlight an intensification of pollution episodes. Moreover, significant discrepancies occur from one year to another, where highest averages show highest standard deviations (Fig. S2). This underlines the need of continuous monitoring over several years periods. Interestingly, no direct link can be drawn between meteorological anomalies and unusual high $PM_{2.5}$ concentrations. Indeed, while the high $PM_{2.5}$ levels observed in February 2012 and March 2012 may be linked to unusual low temperatures, exceptionally high temperatures can also be associated with high $PM_{2.5}$ concentrations. This has to be related to the seasonal variability of sources, origins and (trans)formation pathways; this being investigated within the following sections, taking advantage of long-term trend analysis, wind regression, diurnal variations, and the analysis of pollution episodes.

Finally, it should be underlined that the Paris region is mostly influenced by winds coming from the Southwest (Fig. 5) sector. This sector is characterized by clean air masses from the Atlantic Ocean with high wind speeds, and is usually associated with low PM concentrations. The Northeast wind sector exhibits a smaller occurrence than previously observed between September 2009 and September 2010 (Supplement of Bressi et al., 2013).

5 Long-term trend and general features

2 year temporal variations of the chemical composition of submicron aerosols (OM, NO_3^-, SO_4^{2-}, NH_4^+, Cl^-, BC_{ff} and BC_{wb}) and ammonia (NH_3) are presented in Fig. 1.

ACPD
14, 24221–24271, 2014

Similarly to Bressi et al. (2013), a clear seasonal pattern is observed here, with highest concentrations observed during winter and early spring while summer periods exhibit the lowest pollution levels (Fig. 6a), which is also consistent with general patterns observed in Northern Europe (Barmpadimos et al., 2012; Waked et al., 2014). Regardless of the season, OM dominates the PM_1 chemical composition, followed by ammonium nitrate whose contribution is highest during spring, a feature that is generally observed for European urban areas (Zhang et al., 2007; Putaud et al., 2010). Figure 6b presents the binned major chemical composition and the frequency per season of data points as a function of PM_1 concentration levels. Contribution of Secondary Inorganic Aerosols (SIA, mostly NO_3^-, SO_4^{2-} and NH_4^+) increases with the increase of PM_1 mass until $50\,\mu g\,m^{-3}$, highlighting the role of inorganic secondary pollution during spring months (Fig. 6b). This well-documented pattern that has already been reported for the region of Paris in several studies (see for instance Sciare et al., 2010; Bressi et al., 2013a). Very interestingly, above $50\,\mu g\,m^{-3}$, organic contribution, as well as wintertime frequency, increases to dominate the chemical composition of the highest measured PM_1 concentrations with an associated increase in BC, a feature which has not been seen during the Megapoli nor the AiRPARiF-Particules projects. There are well defined occurrences of high concentrations (~ 150 data points of 30 min) suggesting sharp pollution events with a limited temporal duration; contradictorily to the $20–50\,\mu g\,m^{-3}$ mass class presenting much more data points that highlight either a higher frequency of sharp events and/or pollution episodes with a longer temporal duration.

We have used here the BC/SO_4 ratio to assess potential transport of pollution. Sulphate mainly forms through heterogeneous processes with a slow kinetic rate and spreads over large scales (Putaud et al., 2004). For that reason, it can be considered as a good indicator of long-range transport assuming minor local SO_2 sources (background annual SO_2 concentrations of about $2\,\mu g\,m^{-3}$ in the region of Paris; AiRPARiF, 2014). On the contrary, Black carbon in the region of Paris shows an important gradient from the city center to regional background (Bressi et al., 2013a) and can be used to better infer local (Paris city) influence at our background station. Although in-

ACPD
14, 24221–24271, 2014

situ sulphate formation may occur (for instance during fog episodes; Healy et al., 2012) and long range transport of BC may be observed over the region of Paris (Healy et al., 2012, 2013), as a whole, the use of the BC/SO_4 ratio may support our study on local vs. regional/transported pollution. As shown in Fig. 7, the BC/SO_4 ratio decreases along with the increase of PM_1 (and thus secondary ions mass fraction), suggesting potential regional/trans-boundary transport, and large-scale pollution episodes, as previously reported by several studies in Northern France (Bessagnet et al., 2005; Sciare et al., 2010; Bressi et al., 2013; Waked et al., 2014; Freutel et al., 2013). Very interestingly, this BC/SO_4 ratio dramatically increases for the highest concentrations, where the concomitant increases of the ångström exponent, of the contribution of BC_{wb} relatively to BC, along with the increase of OM and wintertime frequency (Fig. 7), suggest intense local/regional wood burning pollution episodes during winter. Moreover, except the single wood-burning episode observed on 5 February 2012 (described in Petit et al., 2014) all these intense Pm pollution peaks ($Pm_1 > 60\,\mu g\,m^{-3}$) also occurred in most of the rural/suburban/urban aiRPaRiF monitoring stations. This pattern underlines homogeneous meteorological conditions over the region of Paris with "local" emissions being measured at a regional scale (within a distance of at least 50 km from the city center).

6 Seasonality and insights on geographical origins

Figure 8 displays the Wind Regression analysis plots for species of interest, naming Om, NO_3^-, SO_4^{2-}, NH_3, BC_{ff} and BC_{wb}.

Overall, OM concentrations do not exhibit a particular dependence on wind direction, the regional background always staying at a significant contribution throughout seasons ($\sim$ 3–6 $\mu g\,m^{-3}$). However, higher OM concentrations occurred in autumn and winter and are associated with very low wind speeds suggesting higher local influence together with higher local wood burning emissions (as previously suggested from Figs. 6b and 7). During summer, OM concentrations are lower (by a factor of $\sim$ 2.2) and show a more homogeneous distribution (e.g. with lower local influences).

ACPD
14, 24221–24271, 2014

As expected, semi-volatile nitrate concentrations are higher during the coldest months (in spring and winter). They are associated with relatively high wind speeds ($\sim 20\,km\,h^{-1}$) coming from the N and NE direction, suggesting significant medium-to-long-range transport of ammonium nitrate during these seasons which is consistent with similar observations reported for the region of Paris (Bressi et al., 2013a; Freutel et al., 2013; Petetin et al., 2013). However, the significant nitrate concentrations observed for all the range of wind speed from the N–NE direction suggest, at least for the lowest wind speed, a significant contribution of the region of Paris. Possible impacts of industrial activities in the Seine estuary (i.e. Rouen, Le Havre), especially during spring, may also be responsible for the noticeable nitrate hotspot observed in the NW sector. In autumn, nitrate concentrations are higher at low wind speeds, in agreement with the fact that traffic emissions are slightly higher in September and October than the rest of the year in Paris (V-Trafic report, 2014), and that BC_{ff} concentrations are also the highest during these months. This is also consistent with a relatively fast nitrate formation mechanism from local NO_x emissions as reported by Petetin et al. (2013).

Sulphate features different behaviour than nitrate, where the non-local origin is much more pronounced. High concentrations are associated with high wind speeds originating from the NNE, leading to the same conclusions as those reported in the literature on the major role of long range transport of this compound (Pay et al., 2012; Bressi et al., 2013b; Petetin et al., 2013; Waked et al., 2014). Petrochemical and shipping activities may explain the observed hotspot in the marine NW sector, especially noticeable in spring, which may be linked with meteorological conditions enhancing ammonium sulphate formation and transport.

The region of Brittany, located less than 300 km West of the region of Paris, is the principal emitter of ammonia in France through intense agricultural activities (http://prtr.ec.europa.eu/DiffuseSourcesair.aspx). However, no clear contribution from this region is observed from our wind regression analysis. This may be partly related to very few occurrences of air masses passing over Brittany and reaching the region of Paris. Despite hotspots from the NE/E in spring, or from the N/NE in winter, no clear wind

ACPD
14, 24221–24271, 2014

sector is directly responsible for high NH_3 concentrations at our station, suggesting a diffuse regional source for this compound.

In Europe, BC_{ff} is assumed to be an excellent tracer of traffic emissions in urban areas (Herich et al., 2011 for instance). Although long range transported BC_{ff} may not be excluded as shown by Healy et al. (2012, 2013), here, wind regression analyses show that high BC_{ff} concentrations occurred at low wind speeds, highlighting the importance of local/regional traffic emissions in the Paris region, especially during the autumn and winter seasons. In spring, a clear distribution over a large range of wind speeds is noticeable in the NNE wind sector. This is consistent with the fact that Paris city is located NNE from our station (e.g. higher contribution of the Paris city plume to measured BC_{ff} concentrations at SiRTa). This is also related to a higher occurrence of this wind sector during spring.

Black Carbon from biomass burning combustion (BC_{wb}) presents a clear seasonal trend similar to Om, with the highest concentrations during cold seasons at low wind speeds, suggesting increasing local influence in wood burning emissions. The lowest boundary layer heights (BLH) observed during wintertime favouring the accumulation of pollutants at ground level together with the large contribution of individual (domestic) wood burning sources homogeneously spread over the region of Paris may explain the significant contribution of regional emissions observed during winter.

Finally, it should be noted that the geographical origin of each investigated chemical constituent remains globally unchanged throughout the year with a well-defined sectorized location. While SIA and BC_{ff} fractions are mainly associated with the NNE sector (coming from Paris City and/or further away), highest OM and BC_{wb} concentrations exhibit strong local NW and SE sectors origins. Various sources of organic matter also contribute to a significant contribution of the (unsectorized) regional background.

ACPD
14, 24221–24271, 2014

7 Weekly diurnal profiles and insight on sources and processes

Near real-time observations over long-term periods offer a unique opportunity to provide robust diurnal profiles for each season. First, Fig. 9 shows the average diurnal profiles of ambient temperatures (Fig. 9a) and BLH (Fig. 9b) across seasons. Weekly diurnal profiles for Om, NO_3^-, NH_4^+, NH_3, BC_{ff} and BC_{wb} are presented for different seasons from hourly averages (Fig. 10). Sulphate variations are not presented and discussed here because they lead to poor daily variations, which are consistent with its mid-to-long range transport origin.

Clear weekly and diurnal patterns can be observed for carbonaceous aerosols. Independently to the investigated season, BC_{ff} presents a well-marked bimodal diurnal profile, with maxima in the morning (starting at 06:00 UTC) and the evening (starting at 17:00). This reflects the proximity of the traffic source (with daily commuting) and dilution in the boundary layer during daytime (Fig. 9b). With an average of 0.61 $\mu g\,m^{-3}$, weekdays exhibit slightly higher concentrations than weekends (0.51 $\mu g\,m^{-3}$ on average). By comparison, the diurnal variability of BC_{wb} is revealed only in autumn and winter, with the combination of enhanced wood burning emissions, low temperatures and BLH (Fig. 9), leading to a unimodal pattern with increasing concentrations after 18:00 UTC. Although individual wood-burning stoves only represent around 5 % of the means of heating in the region of Paris, they contribute to almost 90 % of PM_{10} residential emissions in the region of Paris (airparif emission inventory for the year 2010; airparif, 2013) and are likely to represent the major contributor to BC_{wb}.

For Om, highest variations (in terms of concentration amplitude) are observed during autumn and winter, with a growing influence of wood-burning heating, as OM concentrations nicely follow BC_{wb} ones. Levels of both compounds during the evening are approximately 20 % higher during weekends than during weekdays. More specifically, low BLH in winter (Fig. 9b) increase measured concentrations, leading, for example, to morning OM peaks that should be linked to traffic emissions. By contrast, the diurnal profile is rather flat with poor temporal variations in summer and is accordance

ACPD
14, 24221–24271, 2014

with the homogeneous geographical distribution from NWR calculation for this season. The lack of decrease in the afternoon during weekdays suggests rapid formation of secondary organic aerosols (SOA) from diverse anthropogenic (traffic for instance, as underlined by Platt et al., 2013 and Nordin et al., 2013) and biogenic sources (Carlton et al., 2009). During spring, OM globally follows the variations of nitrate, highlighting fast displacements of gas-particle equilibriums of semi-volatile material due to meteorological conditions. Some peaks are observed some days during the night, which could underline the residual contribution of wood burning emissions in March and April.

For SIA, nitrate and ammonium display very similar diurnal and weekly profiles, illustrating the importance of ammonium nitrate by comparison with ammonium sulphate. Both compounds display well-marked diurnal profiles with maximum at night (especially in autumn and winter) and/or early morning (especially in spring and summer), which has to be related to the enhancement of ammonium nitrate formation under low temperature and/or high relative humidity. The temporal variations of the two compounds can also be linked to the one of ammonia. For instance, during summertime, ammonia presents a unimodal diurnal profiles, with highest values around noon, and nicely follows temperature (Fig. 9a), in good agreement with previous studies (Bari et al., 2003; Lin et al., 2006). This phenomenon is exactly opposite to the variations of ammonium and nitrate exhibiting unimodal pattern with highest concentrations during the night. Meteorological conditions can then fully control the formation/partitioning of SIA as well as ammonia concentration during summer.

Interestingly however, ammonia shows different profiles as a function of the season. In particular, during springtime, this compound displays a clear bimodal profile, with a morning and an evening peak, concomitant with traffic emissions and that come over elevated regional background levels due to the use of nitrogen-containing fertilizers in this period of the year. However, this bimodal pattern is not observed during the summer and winter seasons, where traffic also occurs. Although traffic-related ammonia has already been reported in urban environments (Edgerton et al., 2007; Pandolfi et al., 2012; Saylor et al., 2010) and several studies raising concerns about uncontrolled

ACPD
14, 24221–24271, 2014

ammonia emissions from De-NO_x systems (Baum et al., 2001; Heeb et al., 2006, 2012 for instance), this spring bimodal profile may also be related to other parameters than traffic emissions. Indeed, as already described by Bussink et al. (1996), emission of ammonia can occur during the evaporation of the morning dew, especially when soils are loaded with fertilizers. The morning decrease observed for ammonia in spring can then be associated with the growing of the mixing depth layer (Fig. 9b) while, in the afternoon ammonia increases may be partly explained by temperature driven gas-phase partitioning changes of ammonium nitrate.

8 PM_1 pollution episodes over the region of Paris

An in-depth characterization of each pollution episodes over the region of Paris is particularly important in the context of mitigation policies which are usually taken at a local scale during these episodes. Such investigation should provide useful information regarding Pm (trans)formation processes and help identifying parameters influencing the temporality of their chemical composition.

Statistical representativeness of pollution episodes (duration and intensity) may be addressed using our long-term datasets. Based on our 2 year dataset, the highest 1 % of observed PM_1 concentrations ($q_{99} \sim 49\,\mu g\,m^{-3}$, representing around 200 data points of 30 min; i.e. approximately 100 h) mostly occur during February, April and November, while persistent pollution episodes ($PM_1 > 20\,\mu g\,m^{-3}$ during at least 3 consecutive days) mostly occur in early Spring. More interestingly, the majority of the highest PM_1 concentrations fall within these persistent pollution episodes. As previously suggested from higher BC/SO_4 ratios (Sect. 5 and Fig. 7), the highest PM_1 concentration peaks are associated with rather local emissions. This result clearly points the contribution of local/regional emissions during persistent pollution episodes. A more detailed analysis (episode-by-episode) is performed in the following to better characterize the local/regional vs. advected Pm pollution during persistent pollution episodes.

ACPD
14, 24221–24271, 2014

Eight persistent pollution episodes ($PM_1 > 20\,\mu g\,m^{-3}$ during at least 3 consecutive days) were detected between mid-2011 to mid-2013 and are displayed in Table 1 and Figs. 12 and 13. Figure 12 shows the averaged PM_1 chemical composition (in $\mu g\,m^{-3}$) for each episode, chronologically numbered, from 1 to 8. Table 1 summarizes key information for each episode. Figure 13 shows air masses origins, wind rose and temporal variations of the chemical composition of each episode. As a general pattern for each episode, the chemical composition of PM_1 is dominated by OM and/or ammonium nitrate. Sulphate presents the highest variability (concentration standard deviation of 53 % over all episodes) compared to OM and nitrate (~ 30 %), possibly suggesting various contributions of advected pollution.

The following provides a thorough description of each episode.

Episode 1 (19 November 2011–24 November 2011): while winds come from the NW and E sectors, 72 h-backtrajectories originate from SSE and exhibit a recirculation over a part of the Northern France. Moreover, along with the BC/SO_4 ratio (3.56; e.g. the highest of all episodes), and a low BLH with no significant variations, the chemical composition is largely dominated by OM (60.8 % of PM_1), suggesting significant local influence. The contribution of BC_{wb} remains insignificant compared to BC_{ff}, which could underline the accumulation in the atmosphere of fossil-fuelled combustion sources (notably illustrated by the very low altitude of the air masses ending on the 21 and 23 November).

Episode 2 (5 February 2012–13 February 2012): this episode presents two distinct phases. At the beginning, air masses come from the SE but originating from the E at low altitudes; along with very low temperatures (below 0 °C all day), high OM and BC concentrations and BC/SO_4 ratio (average of 22.6 and $0.6\,\mu g\,m^{-3}$, and 2.7, respectively from 5 to 8 February). This is related to an intense local wood-burning episode, already thoroughly described in Petit et al. (2014). Then, from the 8 February, winds and air masses originate from NNE and secondary inorganic ions, especially ammonium nitrate, dominate the chemical composition. The associated wind speed may un-

ACPD
14, 24221–24271, 2014

derline mid- to long-range transport, although the impact of the Paris plume cannot be excluded here.

Episode 3 (29 February 2012–3 March 2012): along with this pollution episode, trajectories have rapidly changed in origin but have remained low in altitude. The RH remained very high, reaching 100 % most of the time. Very interestingly, concentrations dropped on 1 March and 3 March during the beginning of the day, coinciding with two stratus lowering fog events. These two fog events occurred during the second half of the night, and evaporated as the sun rose. The influence of fogs regarding the chemical transformation of PM_1 is notably highlighted by higher sulphate concentrations just after the evaporation of the first fog (and also when trajectories flew over the English Channel and Belgium), which could suggest transported SO_2 and oxidation over the region of Paris enhanced by fast fog processing (Kai et al., 2007; Rengarajan et al., 2011).

Episode 4 (12 March 2012–17 March 2012): winds have originated from all directions (but mostly from NNE) suggesting anticyclonic conditions. The first half of the period exhibits rather stable chemical composition (dominated by ammonium nitrate) and clear diurnal variations of RH, T and BHL. Then, after 15 March, daily amplitudes of the following 3 meteorological parameters increased: T reached 20 °C, RH 30 % and BHL 1000 m, compared to the first half where they reached 15 °C, 50 % and 600 m, respectively. This caused rapid decreases of concentrations, due to higher temperature amplitudes enhancing the gas partitioning of semi-volatile material, and an increase of BLH allowing the dilution of atmospheric pollutants.

Episode 5 (23 March 2012–26 March 2013): air masses originated from the NE to the E, and winds from the N to the NE. This episode is characterized by the strong diurnal variation of OM and ammonium nitrate, due the high amplitude of the BLH and temperatures going above 15 °C, similarly to the previous episode. The high average BC/SO_4 ratio (2.37) is not representative of its temporality; the highest values are observed for lowest PM concentrations (26 March afternoon). With this exception, low

ACPD
14, 24221–24271, 2014

BC/SO_4 values (< 1), and the chemical composition dominated by ammonium nitrate suggest mid and/or long-range transport.

Episode 6 (28 March 2012–31 March 2012): it exhibits the same behaviour than episode 5 with a clear medium-to-long range origin pattern (wind speed $\sim 10\,km\,h^{-1}$, chemical composition dominated by ammonium nitrate), but with backtrajectories coming from NW/NE. Low altitude of backtrajectories illustrate the accumulation of pollutants along the trajectory of the air masses. However, the BC peak on the 30 March morning (the high BC_{ff} fraction suggests traffic emissions) could underline an influence of the Paris plume.

Episode 7 (16 January 2013–21 January 2013): air masses display a coiling pattern around Northern France. The BC/SO_4 ratio, remaining lower than 1, suggests advected pollution. However, the strong variability of BC_{wb} illustrates a significant influence of wood-burning emissions. No BHL data are available during this episode, but the altitude of backtrajectories may underline a more important dilution of the pollution.

Episode 8 (1 April 2013–8 April 2013): this episode actually started in 22 March, but no ACSM data were available at that time; however, meteorological conditions from 22 March to 1 April were very similar, notably in terms of wind speeds and direction. It is characterized by air masses originating from the NE and a very low BC/SO_4 ratio, illustrating a typical case of advected secondary pollution, clearly dominated by ammonium nitrate and sulphate.

Overall, the observed variability, in terms of meteorological conditions, air mass origins, and chemical composition illustrates the variety of persistent pollution episodes, in terms of PM sources and different geographical origins. The BC/SO_4 ratio has shown to represent a useful tool to assess the local/regional/advected dimension of a specific pollution episode. Indeed, high ratios (≥ 2) are usually associated with accumulation of local/regional emissions, while very low ratios (≤ 0.5) are more representative of secondary advected pollutants. Ratios within this range should then be associated with a combined influence of regional and advected pollution. Finally, artefact-free ACSM data have shown to be adequate to document semi-volatile aerosols (ammonium ni-

ACPD
14, 24221–24271, 2014

trate and a fraction of OM), which strongly contribute to PM_1 during persistent pollution episodes, and real-time measurements allow to illustrate the close interactions between the chemical composition and meteorological parameters influencing its temporality.

9 Conclusions

The chemical composition of submicron (PM_1) aerosols was continuously monitored in near real-time at a regional background site of the region of Paris between June 2011 and May 2013 using a combination of an ACSM and an Aethalometer. The obtained 2 year dataset allows to appraise the robustness of ACSM measurements over several month periods, as well as Aethalometer measurements and BC source apportionment.

Non-parametric Wind Regression calculations has been performed for each season and provided useful information regarding the geographical origin of PM_1 chemical constituents. SIA, in particular ammonium sulphate, show a clear advected pattern, leading to a uniform signal over large scales. Ammonium nitrate also exhibits a significant contribution of regional and local emissions. The highest concentrations of OM were identified as having a major local origin, while regional background OM concentrations remain significant, especially in spring and summer. The region of Brittany (Western France), the major hotspot of ammonia in France, seems to have little influence on the concentrations of this species at our station in the region of Paris; overall regional background concentrations of ammonia dominate, especially in Spring. Similarly to OM, wintertime BC_{wb} concentrations are mainly from local emissions from domestic heating although a noticeable regional background is still observed for this tracer of wood burning. As expected, BC_{ff} shows a clear local (nearby) origin, as well as contribution from the Paris city plume, and remains fairly constant throughout seasons, due to its regional traffic origin.

Such near real-time observations over long-term periods offer a unique opportunity to provide robust diurnal profiles for each season. For instance, diurnal profiles of semi-

ACPD
14, 24221–24271, 2014

volatile nitrate aerosols were observed in different seasons with temperatures favouring its partitioning into the particulate phase in the morning and in the gas phase in the afternoon. No clear contribution of traffic could be proven regarding ammonia variability, and the regional background seems to prevail.

All the persistent pollution episodes ($PM_1 > 20\,\mu g\,m^{-3}$ during at least 3 consecutive days) which occurred between 2011 and 2013 were carefully examined showing different meteorological conditions, sources and geographical origins making difficult to draw general rules for these episodes. The BC/SO_4 ratio was used here to better separate local/regional (BC dominated) vs. advected (SO_4 dominated) contributions and showed that, with very few exceptions, most of these persistent episodes were dominated by medium-to-long range transported pollution. However, it is interesting to note that the majority of the highest (time-limited) PM_1 concentrations (30 min ACSM data points with $PM_1 > 50\,\mu g\,m^{-3}$) fell within these persistent pollution episodes and were characterized by a significant local/regional contribution (high BC/SO_4 ratios). This result, obtained with real-time measurements, may offer new perspectives in the definition and the evaluation of the effectiveness of local mitigation policies such as emergency measures (traffic or wood burning restrictions, for instance) taken to improve air quality during pollution events.

In conclusion, these first 2 year quality-controlled measurements of ACSM clearly demonstrate their great potential to monitor on a long term basis aerosol sources and their geographical origin and provide strategic information in near real-time during pollution episodes. They also support the capacity of the ACSM to be proposed as a robust and credible alternative to filter-based sampling techniques for long term monitoring strategies. The networking of such instrumentation (ACSM and BC) throughout Europe – as currently being built up within the European ACTRIS program – will certainly offers tremendous opportunities for modeling studies in order to improve prevision models, as well as large scale spatially and temporally resolved source apportionment studies of organic aerosols using the high potential of ACSM organic fragments.

ACPD
14, 24221–24271, 2014

The Supplement related to this article is available online at doi:10.5194/acpd-14-24221-2014-supplement.

Acknowledgements. The research leading to the these results has received funding from INERIS, CNRS, CEA, the French SOERE-ORAURE network, the European Union Seventh Framework Program (FP7/2007-2013) project ACTRIS under grant agreement n° 262254, the DIM-R2DS program for the funding of the ACSM equipment, the PRIMEQUAL-PREQUALIF and ADEME-REBECCA programs for the long term observations of Black Carbon at SIRTA.

References

Aiken, A. C., Salcedo, D., Cubison, M. J., Huffman, J. A., DeCarlo, P. F., Ulbrich, I. M., Docherty, K. S., Sueper, D., Kimmel, J. R., Worsnop, D. R., Trimborn, A., Northway, M., Stone, E. A., Schauer, J. J., Volkamer, R. M., Fortner, E., de Foy, B., Wang, J., Laskin, A., Shutthanandan, V., Zheng, J., Zhang, R., Gaffney, J., Marley, N. A., Paredes-Miranda, G., Arnott, W. P., Molina, L. T., Sosa, G., and Jimenez, J. L.: Mexico City aerosol analysis during MILAGRO using high resolution aerosol mass spectrometry at the urban supersite (T0) – Part 1: Fine particle composition and organic source apportionment, Atmos. Chem. Phys., 9, 6633–6653, doi:10.5194/acp-9-6633-2009, 2009.

Appel, B. R., Tokiwa, Y., Haik, M., and Kothny, E. L.: Artifact particulate sulphate and nitrate formation on filter media, Atmos. Environ., 18, 409–416, 1984.

Arguez, A. and Vose, R. S.: The definition of the standard WMO climate normal: the key to deriving alternative climate normals, B. Am. Meteorol. Soc., 92, 699–704, doi:10.1175/2010BAMS2955.1, 2011.

Bari, A., Ferraro, V., Wilson, L. R., Luttinger, D., and Husain, L.: Measurements of gaseous HONO, HNO_3, SO_2, HCl, NH_3, particulate sulphate and $PM_{2.5}$ in New York, NY, Atmos. Environ., 37, 2825–2835, doi:10.1016/S1352-2310(03)00199-7, 2003.

Barmpadimos, I., Keller, J., Oderbolz, D., Hueglin, C., and Prévôt, A. S. H.: One decade of parallel fine ($PM_{2.5}$) and coarse (PM_{10}–$PM_{2.5}$) particulate matter measurements in Europe: trends and variability, Atmos. Chem. Phys., 12, 3189–3203, doi:10.5194/acp-12-3189-2012, 2012.

ACPD
14, 24221–24271, 2014

Baum, M. M., Kiyomiya, E. S., Kumar, S., Lappas, A. M., Kapinus, V. A., and Lord, H. C.: Multicomponent remote sensing of vehicle exhaust by dispersive absorption spectroscopy. 2. Direct on-road ammonia measurements, Environ. Sci. Technol., 35, 3735–3741, doi:10.1021/es002046y, 2001.

Bond, T. C. and Bergstrom, R. W.: Light absorption by carbonaceous particles: an investigative review, Aerosol Sci. Tech., 40, 27–67, doi:10.1080/02786820500421521, 2006.

Bressi, M., Sciare, J., Ghersi, V., Bonnaire, N., Nicolas, J. B., Petit, J.-E., Moukhtar, S., Rosso, A., Mihalopoulos, N., and Féron, A.: A one-year comprehensive chemical characterisation of fine aerosol ($PM_{2.5}$) at urban, suburban and rural background sites in the region of Paris (France), Atmos. Chem. Phys., 13, 7825–7844, doi:10.5194/acp-13-7825-2013, 2013.

Bussink, D. W., Harper, L. A., and Corré, W. J.: Ammonia transport in a temperate grassland: II. Diurnal fluctuations in response to weather and management conditions, Agron. J., 88, 621–626, 1996.

Cavalli, F., Viana, M., Yttri, K. E., Genberg, J., and Putaud, J.-P.: Toward a standardised thermal-optical protocol for measuring atmospheric organic and elemental carbon: the EUSAAR protocol, Atmos. Meas. Tech., 3, 79–89, doi:10.5194/amt-3-79-2010, 2010.

Cheng, Y., He, K. B., Duan, F. K., Zheng, M., Ma, Y. L., and Tan, J. H.: Positive sampling artifact of carbonaceous aerosols and its influence on the thermal-optical split of OC/EC, Atmos. Chem. Phys., 9, 7243–7256, doi:10.5194/acp-9-7243-2009, 2009.

Chow, J. C., Watson, J. G., Mauderly, J. L., Costa, D. L., Wyzga, R. E., Vedal, S., Hidy, G. M., Altshuler, S. L., Marrack, D., Heuss, J. M., Wolff, G. T., Pope, C. A., and Dockery, D. W.: Health effects of fine particulate air pollution: lines that connect, J. Air Waste Manag., 56, 1368–1380, 2006.

Collaud Coen, M., Weingartner, E., Apituley, A., Ceburnis, D., Fierz-Schmidhauser, R., Flentje, H., Henzing, J. S., Jennings, S. G., Moerman, M., Petzold, A., Schmid, O., and Baltensperger, U.: Minimizing light absorption measurement artifacts of the Aethalometer: evaluation of five correction algorithms, Atmos. Meas. Tech., 3, 457–474, doi:10.5194/amt-3-457-2010, 2010.

Cowen, K., Sumner, A. L., Dinhal, A., Riggs, K., and Willenberg, Z.: Environmental Technology Verification Report, Mechatronics Instruments BV AiRRmonia Ammonia Analyzer, available at: http://www.epa.gov/etv/pubs/01_vr_airrmonia.pdf (last access: 16 September 2014), 2004.

ACPD
14, 24221–24271, 2014

Crippa, M., Canonaco, F., Slowik, J. G., El Haddad, I., DeCarlo, P. F., Mohr, C., Heringa, M. F., Chirico, R., Marchand, N., Temime-Roussel, B., Abidi, E., Poulain, L., Wiedensohler, A., Baltensperger, U., and Prévôt, A. S. H.: Primary and secondary organic aerosol origin by combined gas-particle phase source apportionment, Atmos. Chem. Phys., 13, 8411–8426, doi:10.5194/acp-13-8411-2013, 2013a.

Crippa, M., DeCarlo, P. F., Slowik, J. G., Mohr, C., Heringa, M. F., Chirico, R., Poulain, L., Freutel, F., Sciare, J., Cozic, J., Di Marco, C. F., Elsasser, M., Nicolas, J. B., Marchand, N., Abidi, E., Wiedensohler, A., Drewnick, F., Schneider, J., Borrmann, S., Nemitz, E., Zimmermann, R., Jaffrezo, J.-L., Prévôt, A. S. H., and Baltensperger, U.: Wintertime aerosol chemical composition and source apportionment of the organic fraction in the metropolitan area of Paris, Atmos. Chem. Phys., 13, 961–981, doi:10.5194/acp-13-961-2013, 2013b.

Crippa, M., El Haddad, I., Slowik, J. G., DeCarlo, P., Mohr, C., Heringa, M. F., Chirico, R., Marchand, N., Sciare, J., Baltensperger, U., and Prevot, A. S. H. :Identification of marine and continental aerosol sources in Paris using high resolution aerosol mass spectrometry, Geophys. Res. Lett., 118, 1950–1963, doi:10.1002/jgrd.50151, 2013c

Dall'Osto, M., Ovadnevaite, J., Ceburnis, D., Martin, D., Healy, R. M., O'Connor, I. P., Kourtchev, I., Sodeau, J. R., Wenger, J. C., and O'Dowd, C.: Characterization of urban aerosol in Cork city (Ireland) using aerosol mass spectrometry, Atmos. Chem. Phys., 13, 4997–5015, doi:10.5194/acp-13-4997-2013, 2013.

Draxler, R.: Hysplit4 User's Guide, available at: http://www.arl.noaa.gov/documents/reports/arl-230.pdf (last access: 14 May 2014), 1999.

Edgerton, E. S., Saylor, R. D., Hartsell, B. E., Jansen, J. J., and Alan Hansen, D.: Ammonia and ammonium measurements from the southeastern United States, Atmos. Environ., 41, 3339–3351, doi:10.1016/j.atmosenv.2006.12.034, 2007.

Favez, O., Cachier, H., Sciare, J., Sarda-Estève, R., and Martinon, L.: Evidence for a significant contribution of wood burning aerosols to $PM_{2.5}$ during the winter season in Paris, France, Atmos. Environ., 43, 3640–3644, 2009.

Favez, O., El Haddad, I., Piot, C., Boréave, A., Abidi, E., Marchand, N., Jaffrezo, J.-L., Besombes, J.-L., Personnaz, M.-B., Sciare, J., Wortham, H., George, C., and D'Anna, B.: Intercomparison of source apportionment models for the estimation of wood burning aerosols during wintertime in an Alpine city (Grenoble, France), Atmos. Chem. Phys., 10, 5295–5314, doi:10.5194/acp-10-5295-2010, 2010.

ACPD
14, 24221–24271, 2014

Freutel, F., Schneider, J., Drewnick, F., von der Weiden-Reinmüller, S.-L., Crippa, M., Prévôt, A. S. H., Baltensperger, U., Poulain, L., Wiedensohler, A., Sciare, J., Sarda-Estève, R., Burkhart, J. F., Eckhardt, S., Stohl, A., Gros, V., Colomb, A., Michoud, V., Doussin, J. F., Borbon, A., Haeffelin, M., Morille, Y., Beekmann, M., and Borrmann, S.: Aerosol particle measurements at three stationary sites in the megacity of Paris during summer 2009: meteorology and air mass origin dominate aerosol particle composition and size distribution, Atmos. Chem. Phys., 13, 933–959, doi:10.5194/acp-13-933-2013, 2013.

Grover, B. D.: Measurement of total $PM_{2.5}$ mass (nonvolatile plus semivolatile) with the filter dynamic measurement system tapered element oscillating microbalance monitor, J. Geophys. Res., 110, D07S03, doi:10.1029/2004JD004995, 2005.

Haeffelin, M., Barthès, L., Bock, O., Boitel, C., Bony, S., Bouniol, D., Chepfer, H., Chiriaco, M., Cuesta, J., Delanoë, J., Drobinski, P., Dufresne, J.-L., Flamant, C., Grall, M., Hodzic, A., Hourdin, F., Lapouge, F., Lemaıtre, Y., Mathieu, A., Morille, Y., Naud, C., Noël, V., O'Hirok, W., Pelon, J., Pietras, C., Protat, A., Romand, B., Scialom, G., and Vautard, R.: SIRTA, a ground-based atmospheric observatory for cloud and aerosol research, Ann. Geophys., 23, 253–275, doi:10.5194/angeo-23-253-2005, 2005.

Henry, R., Norris, G. A., Vedantham, R., and Turner, J. R.: Source region identification using kernel smoothing, Environ. Sci. Technol., 43, 4090–4097, doi:10.1021/es8011723, 2009.

IARC: Outdoor air pollution a leading environmental cause of cancer deaths, press release n° 221, available at: http://www.iarc.fr/fr/media-centre/iarcnews/pdf/pr221_E.pdf (last access: 16 September 2014), 2013.

Janssen, N. A., Hoek, G., Simic-Lawson, M., Fischer, P., van Bree, L., ten Brink, H., Keuken, M., Atkinson, R. W., Anderson, H. R., Brunekreef, B., and Cassee, F. R.: Black carbon as an additional indicator of the adverse health effects of airborne particles compared with PM_{10} and $PM_{2.5}$, Environ. Health Persp., 119, 1691–1699, 2011.

Jayne, J. T., Leard, D. C., Zhang, X., Davidovits, P., Smith, K. S., Kolb, C. E., and Worsnop, D. R.: Development of an aerosol mass spectrometer for size and composition analysis of submicron particles, Aerosol Sci. Tech., 33, 49–70, 2000.

Jimenez, J. L., Canagaratna, M. R., Donahue, N. M., Prevot, A. S. H., Zhang, Q., Kroll, J. H., DeCarlo, P. F., Allan, J. D., Coe, H., Ng, N. L., Aiken, A. C., Docherty, K. S., Ulbrich, I. M., Grieshop, A. P., Robinson, A. L., Duplissy, J., Smith, J. D., Wilson, K. R., Lanz, V. A., Hueglin, C., Sun, Y. L., Tian, J., Laaksonen, A., Raatikainen, T., Rautiainen, J., Vaattovaara, P., Ehn, M., Kulmala, M., Tomlinson, J. M., Collins, D. R., Cubison, M. J., Dunlea, E. J.,

ACPD
14, 24221–24271, 2014

Huffman, J. A., Onasch, T. B., Alfarra, M. R., Williams, P. I., Bower, K., Kondo, Y., Schneider, J., Drewnick, F., Borrmann, S., Weimer, S., Demerjian, K., Salcedo, D., Cottrell, L., Griffin, R., Takami, A., Miyoshi, T., Hatakeyama, S., Shimono, A., Sun, J. Y., Zhang, Y. M., Dzepina, K., Kimmel, J. R., Sueper, D., Jayne, J. T., Herndon, S. C., Trimborn, A. M., Williams, L. R., Wood, E. C., Middlebrook, A. M., Kolb, C. E., Baltensperger, U., and Worsnop, D. R.: Evolution of organic aerosols in the atmosphere, Science, 326, 1525–1529, doi:10.1126/science.1180353, 2009.

Kai, Z., Yuesi, W., Tianxue, W., Yousef, M., and Frank, M.: Properties of nitrate, sulphate and ammonium in typical polluted atmospheric aerosols (PM_{10}) in Beijing, Atmos. Res., 84, 67–77, doi:10.1016/j.atmosres.2006.05.004, 2007.

Lack, D. A., Cappa, C. D., Covert, D. S., Baynard, T., Massoli, P., Sierau, B., Bates, T. S., Quinn, P. K., Lovejoy, E. R., and Ravishankara, A. R.: Bias in filter-based aerosol light absorption measurements due to organic aerosol loading: evidence from ambient measurements, Aerosol Sci. Tech., 42, 1033–1041, doi:10.1080/02786820802389277, 2008.

Lin, Y., Cheng, M., Ting, W., and Yeh, C.: Characteristics of gaseous HNO_2, HNO_3, NH_3 and particulate ammonium nitrate in an urban city of Central Taiwan, Atmos. Environ., 40, 4725–4733, doi:10.1016/j.atmosenv.2006.04.037, 2006.

Middlebrook, A. M., Bahreini, R., Jimenez, J. L., and Canagaratna, M. R.: Evaluation of composition-dependent collection efficiencies for the aerodyne aerosol mass spectrometer using field data, Aerosol Sci. Tech., 46, 258–271, doi:10.1080/02786826.2011.620041, 2012.

Ng, N. L., Herndon, S. C., Trimborn, A., Canagaratna, M. R., Croteau, P. L., Onasch, T. B., Sueper, D., Worsnop, D. R., Zhang, Q., and Sun, Y. L.: An aerosol chemical speciation monitor (ACSM) for routine monitoring of the composition and mass concentrations of ambient aerosol, Aerosol Sci. Tech., 45, 780–794, 2011.

Nussbaumer, T., Czasch, C., Klippel, N., Johansson, L., and Tullin, C.: Particulate emissions from biomass combustion in IEA countries, available at: http://www.vbt.uni-karlsruhe.de/index.pl/themen/mahe_wirbel/literatur/Wood-Single-Aspects/Emissions/Partikulate-Emissions-from-Biomass-Combustion-in-IEA-Countries_Nussbaumer_IEA_2008.pdf (last access: 11 June 2014), 2008.

Olson, D. A., Vedantham, R., Norris, G. A., Brown, S. G., and Roberts, P.: Determining source impacts near roadways using wind regression and organic source markers, Atmos. Environ., 47, 261–268, doi:10.1016/j.atmosenv.2011.11.003, 2012.

ACPD
14, 24221–24271, 2014

Pancras, J. P., Vedantham, R., Landis, M. S., Norris, G. A., and Ondov, J. M.: Application of EPA unmix and nonparametric wind regression on high time resolution trace elements and speciated mercury in Tampa, Florida aerosol, Environ. Sci. Technol., 45, 3511–3518, doi:10.1021/es103400h, 2011.

Pandolfi, M., Amato, F., Reche, C., Alastuey, A., Otjes, R. P., Blom, M. J., and Querol, X.: Summer ammonia measurements in a densely populated Mediterranean city, Atmos. Chem. Phys., 12, 7557–7575, doi:10.5194/acp-12-7557-2012, 2012.

Pathak, R., Yao, X., and Chan, C.: Sampling artifacts of acidity and ionic species in $PM_{2.5}$, Environ. Sci. Technol., 38, 254–259, doi:10.1021/es0342244, 2004.

Petit, J.-E., Favez, O., Sciare, J., Canonaco, F., Croteau, P., Močnik, G., Jayne, J., Worsnop, D., and Leoz-Garziandia, E.: Submicron aerosol source apportionment of wintertime pollution in Paris, France by Double Positive Matrix Factorization (PMF_2) using Aerosol Chemical Speciation Monitor (ACSM) and multi-wavelength Aethalometer, Atmos. Chem. Phys. Discuss., 14, 14159–14199, doi:10.5194/acpd-14-14159-2014, 2014.

Pope, C. A. and Dockery, D. W.: Health effects of fine particulate air pollution: lines that connect, J. Air Waste Manag., 56, 709–742, doi:10.1080/10473289.2006.10464485, 2006.

Putaud, J.-P., Raes, F., Van Dingenen, R., Brüggemann, E., Facchini, M.-C., Decesari, S., Fuzzi, S., Gehrig, R., Hüglin, C., Laj, P., Lorbeer, G., Maenhaut, W., Mihalopoulos, N., Müller, K., Querol, X., Rodriguez, S., Schneider, J., Spindler, G., Brink, H. ten, Tørseth, K., and Wiedensohler, A.: A European aerosol phenomenology – 2: Chemical characteristics of particulate matter at kerbside, urban, rural and background sites in Europe, Atmos. Environ., 38, 2579–2595, doi:10.1016/j.atmosenv.2004.01.041, 2004.

Ramgolam, K., Favez, O., Cachier, H., Gaudichet, A., Marano, F., Martinon, L., and Baeza-Squiban, A.: Size-partitioning of an urban aerosol to identify particle determinants involved in the proinflammatory response induced in airway epithelial cells, Part. Fibre Toxicol., 6, doi:10.1186/1743-8977-6-10, 2009.

Rengarajan, R., Sudheer, A. K., and Sarin, M. M.: Wintertime $PM_{2.5}$ and PM_{10} carbonaceous and inorganic constituents from urban site in western India, Atmos. Res., 102, 420–431, doi:10.1016/j.atmosres.2011.09.005, 2011.

Sandradewi, J., Prévôt, A. S. H., Szidat, S., Perron, N., Alfarra, M. R., Lanz, V. A., Weingartner, E., and Baltensperger, U.: Using aerosol light absorption measurements for the quantitative determination of wood burning and traffic emission contributions to particulate matter, Environ. Sci. Technol., 42, 3316–3323, doi:10.1021/es702253m, 2008.

ACPD
14, 24221–24271, 2014

Saylor, R. D., Edgerton, E. S., Hartsell, B. E., Baumann, K., and Hansen, D. A.: Continuous gaseous and total ammonia measurements from the southeastern aerosol research and characterization (SEARCH) study, Atmos. Environ., 44, 4994–5004, doi:10.1016/j.atmosenv.2010.07.055, 2010.

Sciare, J., Sarda-estève, R., Favez, O., Cachier, H., Aymoz, G., and Laj, P.: Nighttime residential wood burning evidenced from an indirect method for estimating real-time concentration of particulate organic matter (POM), Atmos. Environ., 42, 2158–2172, 2008.

Sciare, J., d'Argouges, O., Zhang, Q. J., Sarda-Estève, R., Gaimoz, C., Gros, V., Beekmann, M., and Sanchez, O.: Comparison between simulated and observed chemical composition of fine aerosols in Paris (France) during springtime: contribution of regional versus continental emissions, Atmos. Chem. Phys., 10, 11987–12004, doi:10.5194/acp-10-11987-2010, 2010.

Sciare, J., d' Argouges, O., Sarda-Estève, R., Gaimoz, C., Dolgorouky, C., Bonnaire, N., Favez, O., Bonsang, B., and Gros, V.: Large contribution of water-insoluble secondary organic aerosols in the region of Paris (France) during wintertime, J. Geophys. Res.-Atmos., 116, D22, doi:10.1029/2011JD015756, 2011.

Takegawa, N., Miyazaki, Y., Kondo, Y., Komazaki, Y., Miyakawa, T., Jimenez, J. L., Jayne, J. T., Worsnop, D. R., Allan, J. D., and Weber, R. J.: Characterization of an Aerodyne Aerosol Mass Spectrometer (AMS): Intercomparison with other aerosol instruments, Aerosol Sci. Tech., 39, 760–770, doi:10.1080/02786820500243404, 2005.

Turpin, B. J., Huntzicker, J. J., and Hering, S. V.: Investigation of organic aerosol sampling artifacts in the Los Angeles Basin, Atmos. Environ., 28, 3061–3071, 1994.

Waked, A., Favez, O., Alleman, L. Y., Piot, C., Petit, J.-E., Delaunay, T., Verlinden, E., Golly, B., Besombes, J.-L., Jaffrezo, J.-L., and Leoz-Garziandia, E.: Source apportionment of PM_{10} in a north-western Europe regional urban background site (Lens, France) using positive matrix factorization and including primary biogenic emissions, Atmos. Chem. Phys., 14, 3325–3346, doi:10.5194/acp-14-3325-2014, 2014.

Weingartner, E., Saathoff, H., Schnaiter, M., Streit, N., Bitnar, B., and Baltensperger, U.: Absorption of light by soot particles: determination of the absorption coefficient by means of aethalometers, J. Aerosol Sci., 34, 1445–1463, 2003.

Yiou, P. and Cattiaux, J.: Contribution of Atmospheric circulation to wet North European summer precipitation of 2012, Am. Meteorol. Soc., available at: http://docs.house.gov/meetings/IF/IF03/20130918/101308/HHRG-113-IF03-20130918-SD011.pdf (last access: 14 May 2014), 2013.

ACPD
14, 24221–24271, 2014

Yu, K., Cheung, Y., Cheung, T., and Henry, R. C.: Identifying the impact of large urban airports on local air quality by nonparametric regression, Atmos. Environ., 38, 4501–4507, doi:10.1016/j.atmosenv.2004.05.034, 2004.

Zechmeister-Boltenstern, S.: Training on NH_3 measurement by wet chemistry techniques, ACTRIS TNA Activity Report, available at: http://www.actris.net/Portals/97/tna/tna%20reports/ACTRIS-TNA_NH3measurementTR-CGritsch.pdf (last access: 16 September 2014), 2010.

Zhang, Q., Stanier, C. O., Canagaratna, M. R., Jayne, J. T., Worsnop, D. R., Pandis, S. N., and Jimenez, J. L.: Insights into the chemistry of new particle formation and growth events in Pittsburgh based on aerosol mass spectrometry, Environ. Sci. Technol., 38, 4797–4809, doi:10.1021/es035417u, 2004.

Zhang, Q., Jimenez, J. L., Canagaratna, M. R., Allan, J. D., Coe, H., Ulbrich, I., Alfarra, M. R., Takami, A., Middlebrook, A. M., Sun, Y. L., Dzepina, K., Dunlea, E., Docherty, K., DeCarlo, P. F., Salcedo, D., Onasch, T., Jayne, J. T., Miyoshi, T., Shimono, A., Hatakeyama, S., Takegawa, N., Kondo, Y., Schneider, J., Drewnick, F., Borrmann, S., Weimer, S., Demerjian, K., Williams, P., Bower, K., Bahreini, R., Cottrell, L., Griffin, R. J., Rautiainen, J., Sun, J. Y., Zhang, Y. M., and Worsnop, D. R.: Ubiquity and dominance of oxygenated species in organic aerosols in anthropogenically-influenced Northern Hemisphere midlatitudes, Geophys. Res. Lett., 34, L13801, doi:10.1029/2007GL029979, 2007.

ACPD
14, 24221–24271, 2014

Table 1. Essential parameters describing the 8 pollution episodes, such as the start and end date, average temperature and relative humidity, fraction dominating the chemical composition (SIA stands for Secondary Inorganic Aerosols), BC-to-SO_4 ratio and main geographical contribution.

Episode #	Start–end date	Temp. (°C)	RH (%)	Chemical composition	BC/SO_4	Geographical contribution
1	19 Nov 2011–24 Nov 2011	8.5	93	OM	3.56	Regional
2	5 Feb 2012–13 Feb 2012	−4.7	71	OM then SIA	0.91	Strong local, then regional and advected
3	29 Feb 2012–3 Mar 2012	8.2	95	SIA	1.12	Strong regional, low advected
4	12 Mar 2012–17 Mar 2012	10.7	78	SIA	0.95	Advected and regional
5	23 Mar 2012–26 Mar 2012	15	48	SIA	2.37	Strong advected, low regional
6	28 Mar 2012–31 Mar 2012	12.3	62	SIA	1.42	Strong advected and regional
7	16 Jan 2012–21 Jan 2012	−3	93	OM and SIA	0.72	Strong regional and advected
8	1 Apr 2013–8 Apr 2013	4.2	64	SIA	0.12	Advected

ACPD
14, 24221–24271, 2014

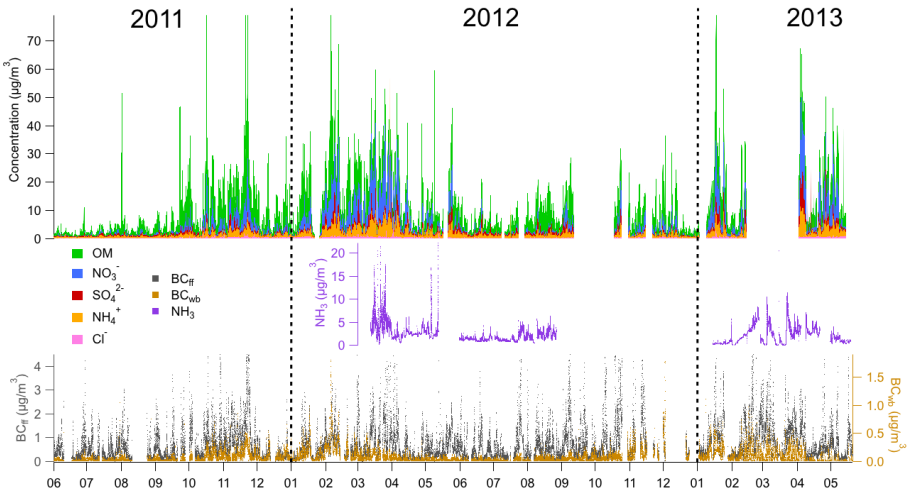

Figure 1. Time series of the major 30 min non-refractory (top, concentrations are aggregated) and 5 min refractory (bottom, concentrations are dissociated) PM_1 chemical constituents, and 5 min ammonia at SIRTA from June 2011 to May 2013. The two large data gaps in October 2012 and March 2013 correspond to two field intensive campaigns during which the ACSM was deployed elsewhere.

ACPD
14, 24221–24271, 2014

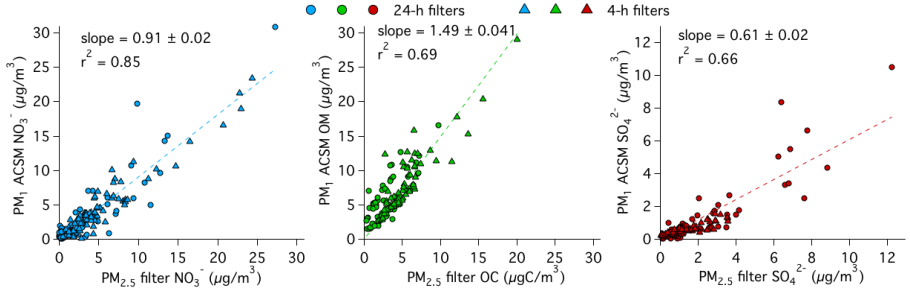

Figure 2. Scatter plot of chemically-speciated ACSM measurements vs. filter analyses for nitrate, organic matter (compared to OC filter-based measurements) and sulphate.

ACPD
14, 24221–24271, 2014

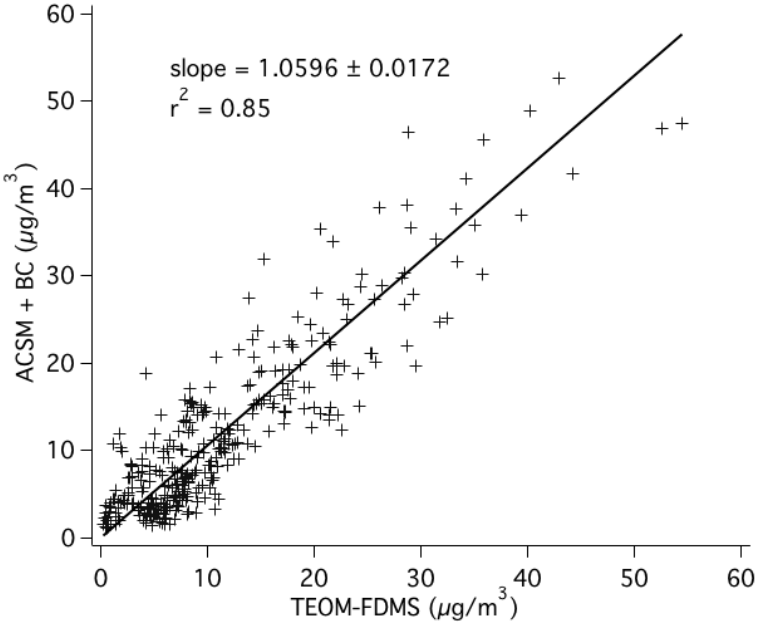

Figure 3. Mass closure exercise between daily averaged reconstructed PM_1 (ACSM + BC) and measured PM_1 by TEOM-FDMS.

ACPD
14, 24221–24271, 2014

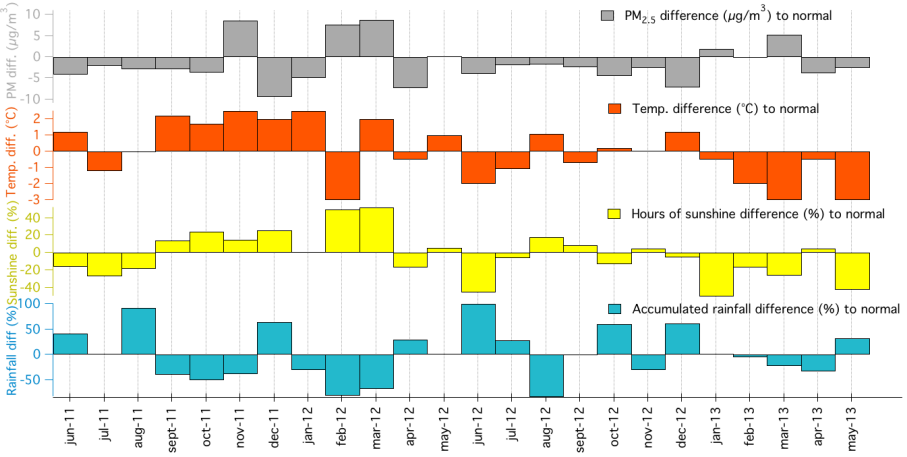

Figure 4. Comparison between observed and average $PM_{2.5}$, temperature, hours of sunshine and accumulated rainfall in the region of Paris.

ACPD
14, 24221–24271, 2014

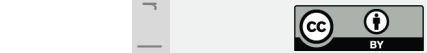

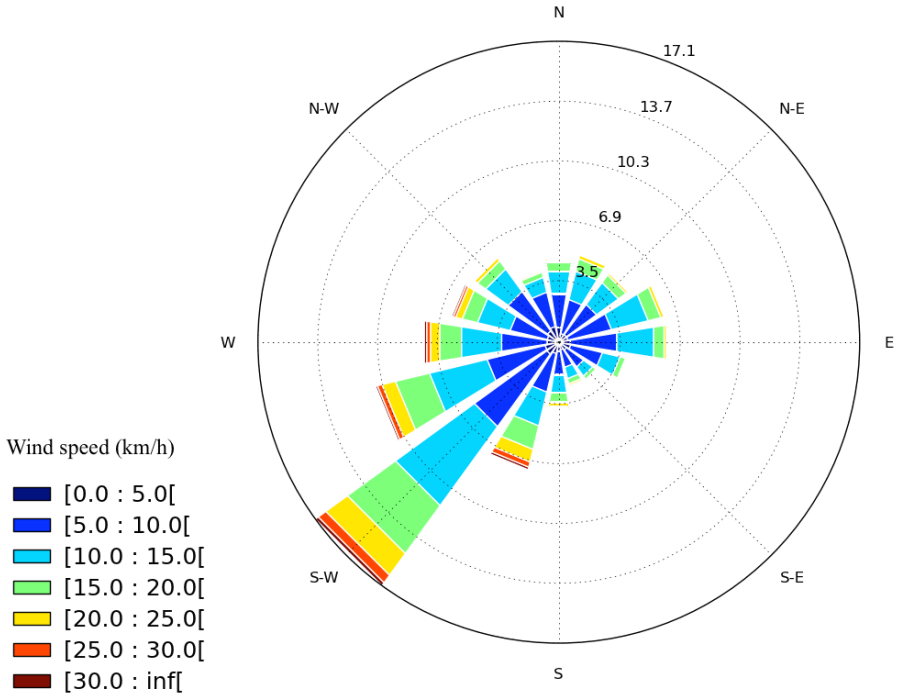

Figure 5. Average wind rose during June, 2011 and June, 2013, the radial axis represents the wind occurrence (in %).

ACPD
14, 24221–24271, 2014

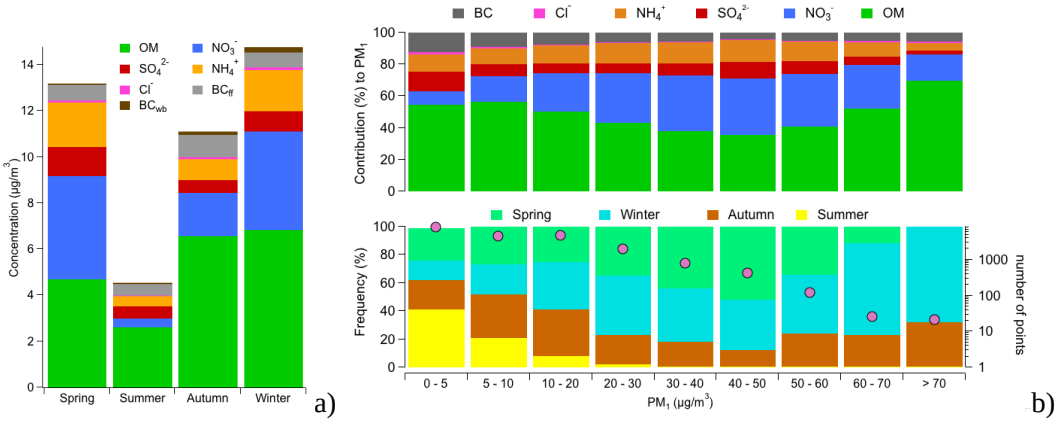

Figure 6. (a) PM_1 chemical composition for different mass classes (top), with the seasonal occurrence frequency and number of points in each bin (bottom) **(b)** seasonal PM_1 chemical composition. Each data point correspond to 1 ACSM (30 min) measurement.

ACPD
14, 24221–24271, 2014

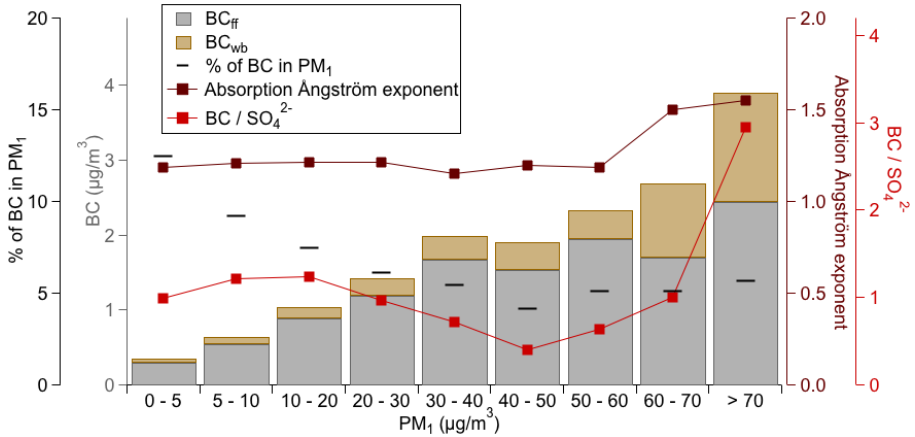

Figure 7. Source contribution to BC, absorption Ångström exponent, BC-SO4 ratio, and contribution of BC to PM_1, depending on PM_1 mass.

ACPD
14, 24221–24271, 2014

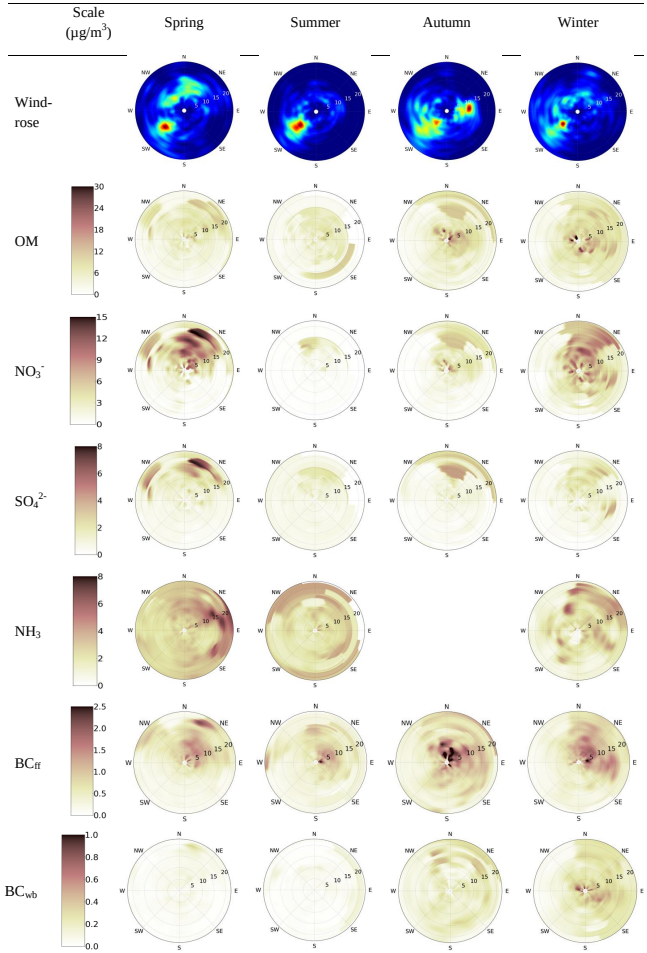

Figure 8. Seasonal NWR plots for the major components of PM_1 and gaseous ammonia. Radial and tangential axes represent the wind direction and speed (km h^{-1}), respectively.

ACPD
14, 24221–24271, 2014

Two years of near real-time chemical composition of submicron aerosols

J.-E. Petit et al.

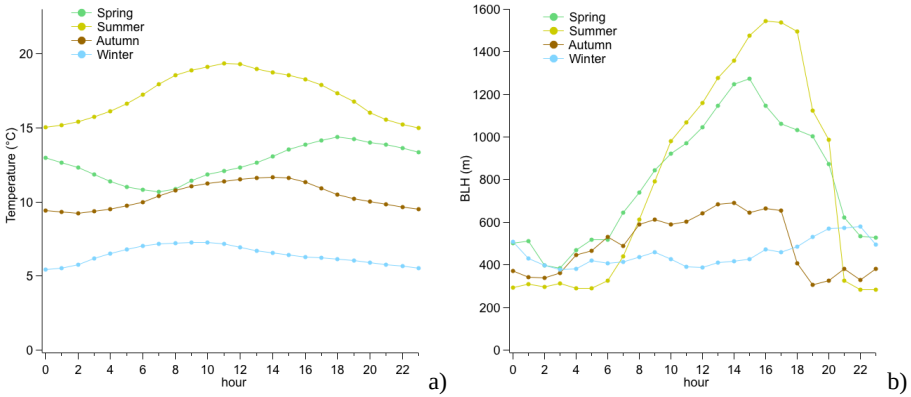

Figure 9. Average diurnal variations by seasons of temperature **(a)** and BLH **(b)**.

ACPD
14, 24221–24271, 2014

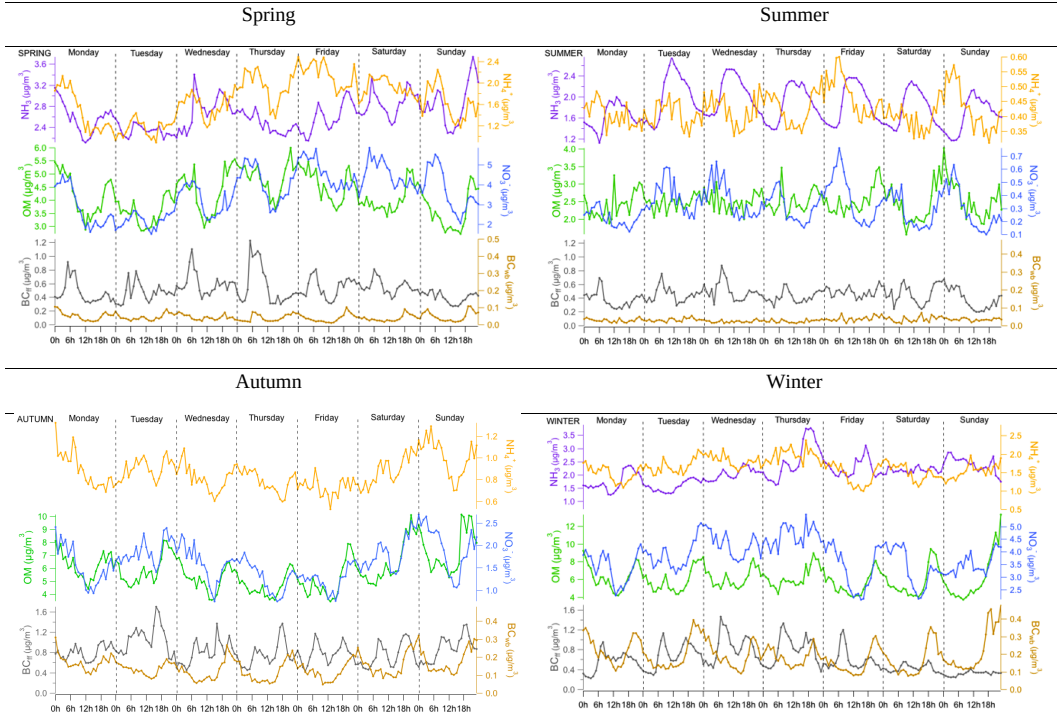

Figure 10. Seasonal weekly diurnal variations of OM (green), NO_3^- (blue), NH_4^+ (dark yellow), NH_3 (purple), BC_{ff} (black) and BC_{wb} (brown).

ACPD
14, 24221–24271, 2014

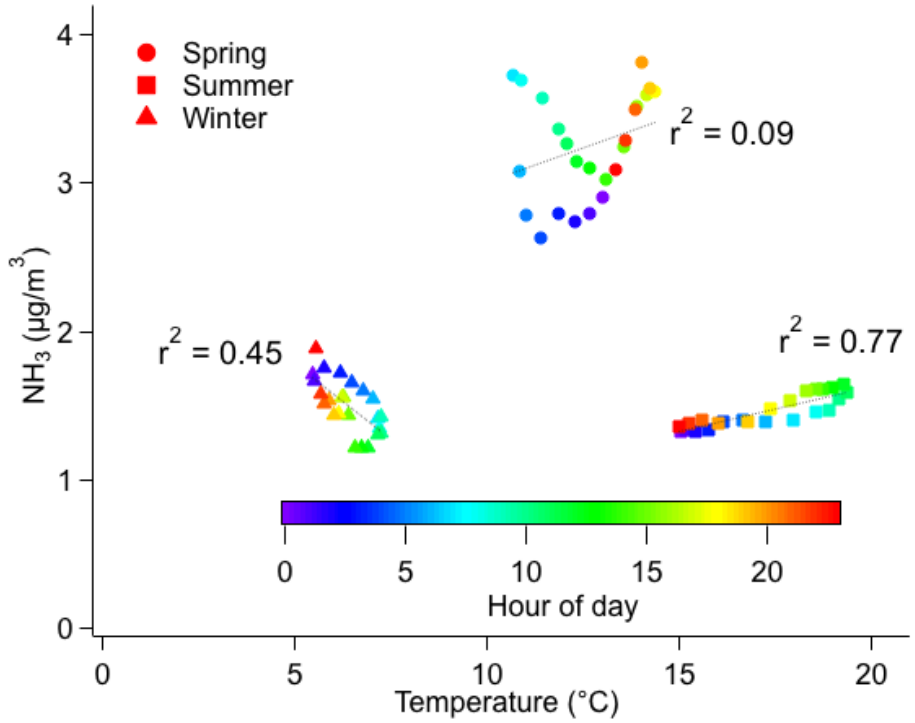

Figure 11. Correlation between ammonia and temperature in spring (circles), summer (squares) and winter (triangles) coloured as a function of the hour of day.

ACPD
14, 24221–24271, 2014

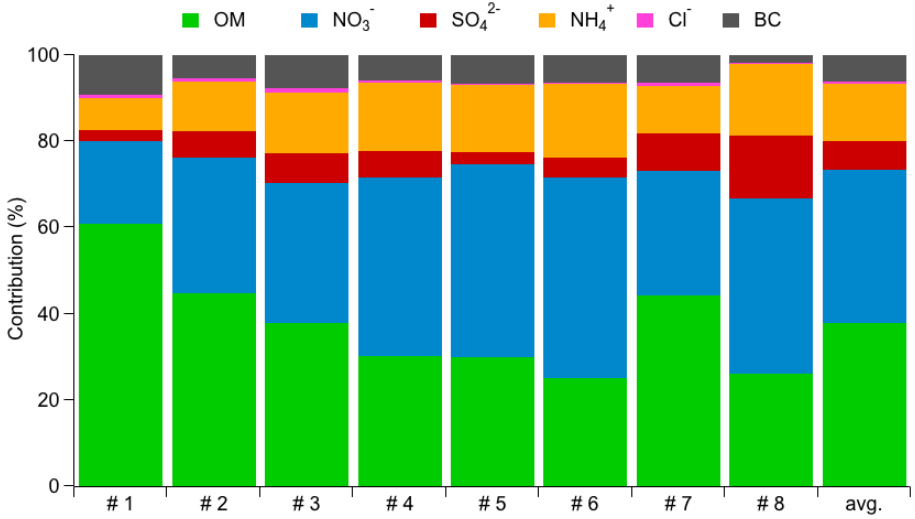

Figure 12. PM_1 chemical composition of the 8 pollution episodes.

ACPD
14, 24221–24271, 2014

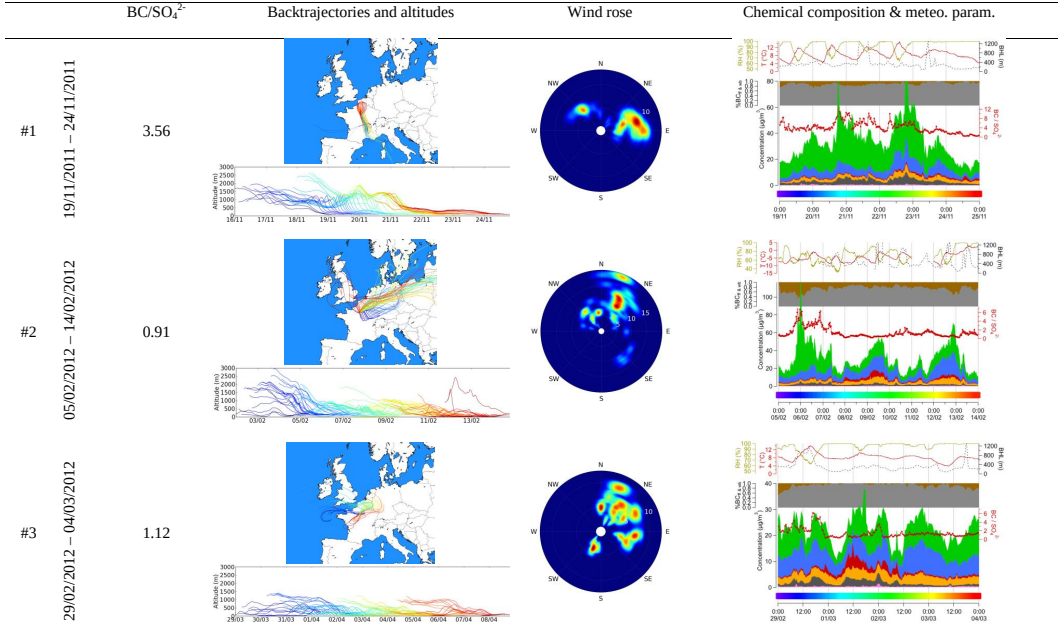

Figure 13. Illustration of meteorological conditions and chemical composition during the 8 pollution episodes. Left graphs represent 72 h-backtrajectories ending at SIRTA at 100 m a.g.l. every 3 h and their altitude; Middle graphs illustrate the wind rose (radial axis in km h^{-1}); Right graphs represent the chemical composition, in µg m^{-3} of submicron particle (organic, nitrate, sulphate, ammonium, chloride and black carbon in green, blue, red, orange, pink and dark grey, respectively), the contribution of traffic and wood-burning to BC, the BC/SO_4^{2-} ratio, and temperature, RH and BLH.

ACPD
14, 24221–24271, 2014

Two years of near real-time chemical composition of submicron aerosols

J.-E. Petit et al.

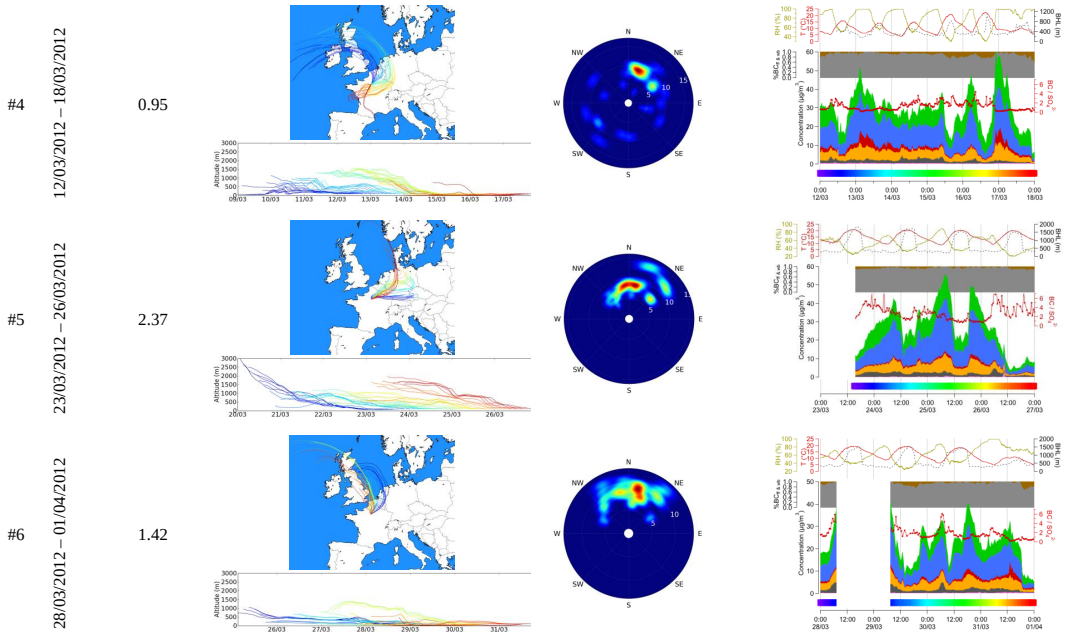

Figure 13. Continued.

ACPD
14, 24221–24271, 2014

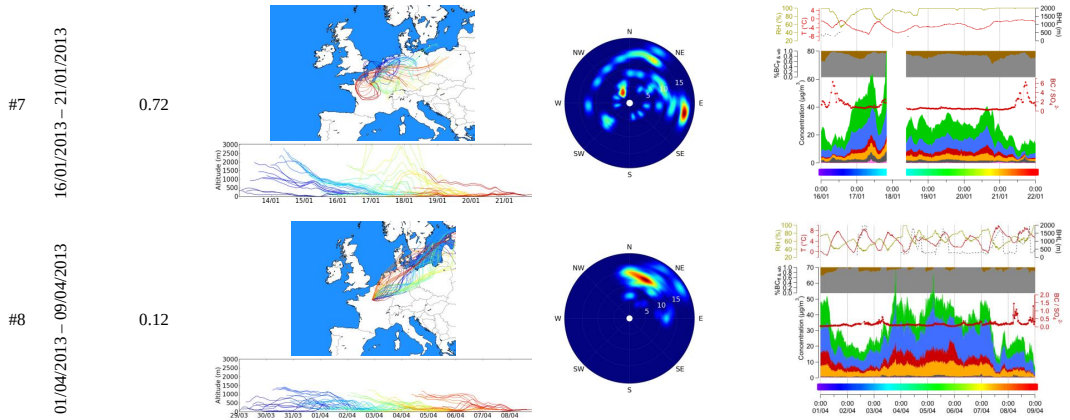

Figure 13. Continued.

ACPD
14, 24221–24271, 2014